Published in final edited form as:
Brain. 2008 April ; 131(0 4): 1123–1133. doi:10.1093/brain/awn004.

Myeloperoxidase-targeted imaging of active inflammatory lesions in murine experimental autoimmune encephalomyelitis

John W. Chen[1,2,*], **Michael O. Breckwoldt**[2], **Elena Aikawa**[2], **Gloria Chiang**[2], and **Ralph Weissleder**[1,2]

[1]Center for Systems Biology, Massachusetts General Hospital, Harvard Medical School, 5404 Building 149, 13th Street, Charlestown, MA 02129

[2]Center for Molecular Imaging Research, Massachusetts General Hospital, Harvard Medical School, 5404 Building 149, 13th Street, Charlestown, MA 02129

Abstract

Inflammatory demyelinating plaques are the pathologic hallmark of active multiple sclerosis and often precede clinical manifestations. Noninvasive early detection of active plaques would thus be crucial in establishing presymptomatic diagnosis and could lead to early preventive treatment strategies. Using murine experimental autoimmune encephalomyelitis as a model of multiple sclerosis, we demonstrate that a prototype paramagnetic myeloperoxidase (MPO) sensor can detect and confirm more, smaller, and earlier active inflammatory lesions in living mice by *in vivo* magnetic resonance imaging (MRI). We show that MPO expression corresponded with areas of inflammatory cell infiltration and demyelination, and higher MPO activity as detected by MPO imaging, biochemical assays, and histopathological analyses correlated with increased clinical disease severity. Our findings present a potential new translational approach for specific noninvasive inflammatory plaque imaging. This approach could be used in longitudinal studies to identify active demyelinating plaques as well as to more accurately track disease course following treatment in clinical trials.

Keywords

myeloperoxidase; neuroinflammation; demyelination; targeted imaging; MRI

Introduction

Multiple sclerosis (MS), the leading cause of nontraumatic neurological disability in young adults (Noseworthy et al., 2000), is characterized by the formation of demyelinating plaques in the central nervous system (CNS) from an immune-mediated inflammatory response induced by lymphocytes, macrophages, and microglia (Bruck, 2005; Frohman et al., 2006; Imitola et al., 2006; Noseworthy et al., 2000). In the active stage of the disease, macrophages/microglia are abundant in perivascular locations (Noseworthy et al., 2000). Inflammatory plaques form early in multiple sclerosis and often precede clinical symptoms

*corresponding author (John W. Chen): chenjo@helix.mgh.harvard.edu, 617-726-5788 (phone), 617-726-5708 (FAX).

(Frohman et al., 2003; Miller et al., 2005). Early diagnosis with prompt treatment has been found to delay relapse (Jacobs et al., 2000) and decrease axonal loss from inflammation (Bruck, 2005; Frohman et al., 2006; Kutzelnigg et al., 2005). Currently, active disease is inferred from contrast enhancement identified on magnetic resonance imaging (MRI). However, it is widely recognized that these MRI techniques have limitations because contrast enhancement reflects breakdown in the blood-brain barrier (BBB) with leakage of paramagnetic chelates rather than active inflammation, and the two may not always correspond. In particular, MS lesions at all stages demonstrate some BBB breakdown (Cotton et al., 2003), and lesions can remain enhanced 1 to 13 weeks after the onset of clinical symptoms (Bruck et al., 1997; Cotton et al., 2003). Furthermore, to be detectable by contrast enhanced MRI, a lesion needs to have significant breakdown of the BBB to allow micromolar accumulation of conventional gadolinium (Gd) agents. However, early demyelinating lesions may only have subtle BBB impairment, insufficient for a large amount of Gd agents to extravasate. As such, contrast-enhanced MRI has been found to underreport active MS lesions (Filippi et al., 1996; Kidd et al., 1999) and correlate poorly with immunological markers (Giovannoni et al., 2000). Therefore, a noninvasive method to detect and confirm acute inflammatory plaques in patients suspected of MS would allow prompt diagnosis and preventive treatment before irreversible disabilities occur.

Myeloperoxidase (MPO), one of the most abundant enzymes secreted by inflammatory cells (Bradley et al., 1982) including neutrophils, macrophages, and microglia, is found in active MS plaques (Nagra et al., 1997). Individuals with higher MPO expression have increased susceptibility to MS (Chataway et al., 1999; Zakrzewska-Pniewska et al., 2004). MPO generates highly reactive molecular moieties, such as hypochlorite, tyrosyl radicals, and aldehydes and can cause local damage and further activate the inflammatory cascade (Heinecke, 1997). MPO would thus be a good imaging target for the detection and confirmation of active inflammation in MS.

In the present study, we use a prototype MPO-activatable paramagnetic sensor (Chen et al., 2006) to show that MPO-targeted MR imaging can increase our ability to detect more and confirm smaller and earlier active demyelinating lesions. When converted by MPO in the presence of hydrogen peroxide (e.g., from NADPH oxidase), the sensor is radicalized and forms oligomers of higher longitudinal relaxivity (R_1), and in addition can covalently bind to proteins, again accompanied by R_1 increases (Figure 1). These MPO-induced chemical changes result in markedly increased MR signal on T1-weighted MRI sequence and improved pharmacokinetics because converted products are locally retained.

Methods

Experimental autoimmune encephalomyelitis (EAE)

The protocol for animal experiments was approved by the institutional animal care committee. SJL female mice 6–10 weeks of age were obtained from Jackson Laboratories (Bar Harbor, ME). A total of 40 SJL mice were used for this study. Five mice were used as controls with sham induction by injecting saline instead of proteolipid protein. EAE in the remaining 35 mice was induced with synthetic proteolipid protein ($PLP_{139–151}$, Axxora, CA) according to Greer et al. (Greer et al., 1996). Briefly, 2 mg of PLP and 8 mg *M. tuberculosis*

H37Ra (Difco, MI) were dissolved in 1 mL H_2O, and then combined with 1 mL of complete Freud's adjuvant (Sigma-Aldrich, MO), and transferred to a 3 mL glass syringe connected to another 3 mL glass syringe via a 20-G needle connector. The content was emulsified by transferring between the two syringes while on ice. Each mouse received 100 μL of the PLP emulsion (25 μL each in the bilateral inguinal and axillary regions). On day 0 and 2, 0.1 μg of pertussinogen dissolved in 200 μL of PBS was injected intravenously via the tail vein. The animals were monitored at least daily with the following clinical grading: 0 = normal, 1 = complete tail limpness with no limb weakness, 2 = hind limb weakness but no obvious paralysis on ambulation, 3 = partial hind limb paralysis, 4 = complete hind limb paralysis, 5 = moribund.

Imaging agents

The chemicals were purchased from Sigma-Aldrich (St. Louis, MO). The MPO-sensitive imaging agent bis-5-hydroxytryptamide-diethylenetriamine-pentaacetate gadolinium (bis-5HT-DTPA(Gd)) was synthesized according to Querol et al.(Querol et al., 2005) Briefly, DTPA-bisanhydride was reacted with serotonin in dimethylformamide in the presence of an excess of triethylamine. The product bis-5HT-DTPA was isolated by recrystallization from methanol and acetone. Complexation with gadolinium was performed in the presence of 1% citric acid (w/w), and purified by high performance liquid chromatography. DTPA(Gd) (Magnevist) was purchased from Berlex Laboratories (Berlex, NJ).

Blood half-life

Six C57BL/6 mice were injected with 100 μCi of ^{111}In-bis-5HT-DTPA. Blood was extracted at 1, 10, 30, 60, 240, 480, and 1400 minutes after injection and radioactivity measured on a 1480 Wizard gamma counter (Perkin-Elmer, MA).

Histopathological analyses

1. Detection of demyelination—Fresh frozen sections of brains were prepared by embedding the tissue in OCT and snap-frozen with isopentane on dry ice. Demyelination of axons was detected with the luxol fast blue stain, which binds to phospholipids of myelin to result in a blue staining. 5 μm Fresh-frozen sections were incubated with 0.1% of luxol fast blue solution at room temperature overnight and differentiated in lithium carbonate and 70% ethyl alcohol. Quantification of demyelination was performed by tracing the areas resistant to the luxol fast blue stain and dividing the resultant area by the total white matter area. The tracing was performed using the software OsiriX (version 2.7.5, www.osirix-viewer.com).

2. Immunohistochemical analyses—5 μm sections of fresh frozen tissues were examined for the presence of myeloperoxidase (rabbit polyclonal antibody; AbCam, MA) and macrophages/microglia (mac-3, BD Biosciences, CA). The avidin-biotin peroxidase method was employed. The reaction was visualized with 3-amino-9-athyl-carbazol substrate (AEC, Sigma Chemical, Mo). Tissue sections from healthy animals were used as controls. Hematoxylin-eosin staining was also performed to study the overall morphology. All sections were also counterstained with hematoxylin. Images were captured with a digital camera (Nikon DXM 1200-F, Nikon Inc., NY).

3. Double immunofluorescence confocal microscopy—To show co-localization of MPO and macrophages/microglia, we performed dual channel fluorescence confocal microscopy. The same antibodies were used as for immunohistochemistry. Secondary antibodies were detected with streptavidin conjugated with Texas Red (MPO) and streptavidin coupled to FITC (Mac-3) (both 1:100, Amersham, NJ) and an avidin/biotin blocking kit (Vector Laboratories, CA) to prevent cross-reaction of the antibodies. A Nikon 80i microscope and an Axiovert 200M inverted confocal microscope (Carl Zeiss, NY) equipped with an LSM Pascal Vario RGB Laser (Arg 458/488/514 nm, HeNE 543 nm, HeNe 633 nm) were used. Summation of projection of all background-corrected slices was produced using the LSM 5 Pascal Software (v 3.2 WS). Final images were colour-coded green for FITC and red for Texas Red.

Western blot analysis

To confirm the presence of MPO in the brains, mice were sacrificed, brains homogenized, and proteins extracted in 1% cetyltrimethylammonium bromide (Sigma-Aldrich, MO) in PBS w/v. The resultant suspension was sonicated for 30 seconds and then underwent three cycles of freeze-thaw in liquid nitrogen. Subsequently, the suspensions were centrifuged at 14,000 rpm for 15 minutes, and the supernatant used for protein analysis (Bicinchoninic acid kit, Sigma-Aldrich, MO). The blots were performed using a monoclonal rabbit anti-MPO (Upstate, CA), 1:1,000 dilution, and a rabbit polyclonal ß-Actin antibody (Abcam, MA), 1:5,000 dilution using chemiluminescence detection. Thirty Og of protein from the samples were loaded and ß-Actin was used as a loading control.

MPO activity assay

To quantify MPO activity and to correlate the activity to clinical disease severity, we performed MPO activity assays according to the method established by Klebanoff et al. (Klebanoff et al., 1984) against guaiacol using a UV/vis spectrometer (Varian Cary 50 Bio UV-Vis spectrometer, CA) at 470 nm. Mouse brains were prepared as described above for Western blot analyses. Forty Og of protein were used for each assay. The units of activity were computed according to the following formula: Activity = $(\Delta OD \times Vt \times 4)/(E \times \Delta t \times Vs)$, where ΔOD = change in absorbance; Vt = total volume; Vs = sample volume; E (extinction coefficient) = $26.6 mM^{-1}$; Δt = change in time.

Imaging

MR imaging was performed using a 4.7 T Bruker Pharmascan MRI scanner with a mouse brain coil under respiration-monitored isoflurane gas anesthesia (Bruker Biosciences, Billerica, MA). Some animals were also imaged on a 7 T Bruker Pharmascan MRI scanner (Bruker Biosciences, Billerica, MA) to demonstrate that the MPO sensor can report MPO activity at higher field strengths due to improved pharmacokinetics after MPO activation, which is independent of field strength. Comparison between MPO imaging and DTPA(Gd) imaging was also performed at the same field strength for each animal. Pre- and post-contrast spin-echo T1-weighted images (TR=800, TE=13, four signal acquired, acquisition time of 6 minutes 57 seconds, matrix size 192×192, field of view 2.5 × 2.5 cm, slice thickness 0.7 mm, and 16 sections were acquired) were obtained after the administration of

0.3 mmol/kg of either agent. Post-contrast imaging was obtained sequentially for at least 60 minutes after contrast administration. To minimize differences resulting from lesion progression between imaging sessions, we randomized the order of the agent administration, with half of the animals administered with the MPO sensor first, and the other half of the animals administered with the conventional agent first. We also only imaged those animals that did not change clinical staging between the imaging periods. Both MPO-imaging and DTPA(Gd) imaging were performed within 24 hours of each other, with a minimum of 6 hours between contrast injections to ensure clearance of the previously injected agent, resulting in an average time between different agent administration of 15.1 hours ± 8.5 hours.

Statistical analysis

Contrast-to-noise ratios (CNR) were computed for each region of interest (ROI) according to the formula: $CNR = (ROI_{lesion} - ROI_{normal\ brain})/SD_{noise}$, where ROI_{lesion} is the ROI of an enhancing lesion, $ROI_{normal\ brain}$ indiates the ROI of an unaffected area of the brain, and SD_{noise} is the standard deviation of noise from an ROI measuring empty space. The resultant curves were compared using the paired permutative Kolmogrov-Smirrnov test, which does not assume normal distributions. A p-value less than 0.05 was considered to be statistically significant.

Comparisons of lesion detection and lesion burden were performed by visually counting the number of and area of enhanced lesions over the entire brain for each mouse by two independent observers blinded to the injected agent (JWC and MOB), and the results were averaged. Only parenchymal lesions were included in the analyses. For volumetric analysis, the area of the lesion was multiplied by the slice thickness to arrive at the lesion volume. The resultant data were analyzed with the student *t*-test. MPO activity assay was also analyzed with the two-tailed student *t*-test. The number of animals used for each part of the study was chosen to achieve 90% power. A p-value less than 0.05 was considered to indicate a statistically significant difference. All results were reported with standard deviation, except where indicated. All statistical computations were performed using a statistical software package (R, version 2.4.1, R Foundation for Statistical Computing, Vienna, Austria).

Results

MPO is present in the brains of MS model mice and correlates with disease severity

Experimental autoimmune encephalomyelitis (EAE) is an animal model of MS most often used in experimental and clinical trials. To determine baseline levels of MPO we performed Western blotting on whole brain specimen of mice with and without EAE. Control mice have negligible MPO heavy chain levels while MPO was markedly up-regulated in EAE mice (Figure 2a). We next assessed MPO enzymatic activity in EAE mice at different stages of disease progression. In control mice, no significant MPO activity was detected in the brain. In EAE mice, MPO activity in the brain was substantially higher (from 4.8 to 55 U/mg of protein, with an average of 26 (SEM 8.2) U/mg of protein). When stratified by clinical staging, there was a statistically significant difference between the MPO activity of stages 0–1 (no limb weakness) and stages 2–3, (with limb weakness) (Figure 2b, p=0.012).

There was increased percent demyelination at increasing clinical disease severity (Figure 2c, R^2=0.93, p=0.0021). When the individual animal's MPO activity was plotted against its corresponding clinical disease stage (Figure 2c), we found a positive correlation (R^2=0.73, p=0.014).

Areas of increased MPO activity colocalized with demyelination and tissue destruction

In EAE mice sacrificed at clinical stages 2 and 3, there were multiple areas of macrophage/microglia accumulation, a finding most pronounced in the cerebellum. Macrophage/microglia accumulated primarily around microvascular structures and contained MPO (Figure 3). In one of the mice a lesion was detected by MPO imaging as early as day 5 after induction in the cerebellum (Figure 3a). The areas of demyelination in the white matter corresponded well to areas identified by MPO and the MR images obtained with the MPO sensor (Figure 3b). Double immunofluorescence labeling (Figure 4a) showed co-localization of MPO positive cells to macrophage/microglial cells, confirming macrophage/microglial cells as the source of MPO. Confocal microscopy (Figure 4b) further demonstrated widespread architectural distortion and loss of normal white matter in areas of macrophage/microglia accumulation and MPO expression (Figure 4b). MPO and inflammatory cells infiltrated not only white matter but also affected the cortex (Figure 3). Similar findings have been reported in mouse, rat, and marmoset monkey EAE models (MacKenzie-Graham et al., 2006; Merkler et al., 2006; Pomeroy et al., 2005; Storch et al., 2006), and in human multiple sclerosis (Kidd et al., 1999; Kutzelnigg et al., 2005).

Active lesions show increased enhancement and retention of the MPO sensor

To determine whether MPO imaging would allow *in vivo* sensing of active inflammation we performed serial comparative MRI studies using the MPO sensor and the conventional agent DTPA(Gd). Similar to previous studies, there was diffuse breakdown in the BBB seen by both DTPA(Gd) and MPO imaging, particularly in the cerebellum and the brainstem (Floris et al., 2004; Seeldrayers et al., 1993). With the conventional contrast agent DTPA(Gd) there was an initial increase and subsequent rapid loss of enhancement over time (Figures 5c), similar as reported clinically. In contradistinction, because of activation by MPO, imaging with bis-5HT-DTPA(Gd) showed higher increase in contrast at the same dosage as DTPA(Gd) and in addition demonstrated prolonged tissue enhancement persisting over at least 60 minutes (Figure 5c). Some representative examples are shown in Figure 5a and 5b where many lesions were detected by MPO imaging but not by conventional contrast enhanced MRI. Delayed MPO images confirmed MPO activation by demonstrating persistent enhancement (examples given by arrows in Figure 5a). Comparing the immediate post contrast images, conventional MRI showed a more diffuse, less well-defined pattern of enhancement (Figure 5b), while MPO imaging demonstrated a more discrete enhancement pattern (Figure 5a) that reflected focal areas of inflammation corresponding to inflamed perivascular lesions histopathologically (Figure 4a). In addition, delayed images demonstrated widespread retained enhancement (Figure 5), indicating more diffuse MPO infiltration, similar to histopathological results (Figure 3). Furthermore, larger lesion volume determined on delayed MPO images correlated with higher MPO activity (R^2=0.72, Figure 5d) and corresponded to higher clinical disease severity (p=0.0052, Figure 5e). Furthermore, enhancing areas measured from MPO imaging correlated better (R^2=0.96, p=0.002, Figure

5f) with percent demyelination than those measured from conventional imaging (R^2=0.65, p=0.098, Figure 5f). Areas of persistent enhancement on MPO imaging thus represented areas with elevated MPO expression and activity, and colocalized to regions of increased inflammation with macrophage/microglia infiltration, demyelination, and disruption of the normal brain structure. Given the short blood half-life of the non-activated MPO-sensitive agent bis-5HT-DTPA(Gd) monomer (5.4 min ± 0.9 min, similar as DTPA(Gd)), the prolonged retention is consistent with MPO-agent activation and protein binding. While there is protein binding once the MPO sensor is activated, resulting in prolonged enhancement, we found that within 6 hours after injection, the MRI signal changes had reverted to background (Figure 5a/b, third animal from the left) potentially allowing for serial/longitudinal imaging.

MPO imaging improves sensitivity of lesion detection

There was consistently improved lesion detection by MPO imaging compared to conventional MRI (Figure 6a). MPO imaging was able to detect more lesions (Figure 6a, p=0.0013) and much smaller lesions (about 40% smaller, p=0.031, Figure 6b). Furthermore, MPO imaging detected lesions at an earlier time point (e.g, Figure 5, third animal from left) where more lesions were detected and confirmed by MPO imaging but not by conventional DTPA(Gd) imaging performed 6 hours later where some of the lesions detected by MPO imaging were either absent or barely perceptible, even retrospectively. Correlative MPO histopathology confirmed the improved imaging sensitiv by MPO imaging (Figure 6c).

Discussion

In the present study, we demonstrate that a small molecule myeloperoxidase substrate can be used to noninvasively image active inflammatory, demyelinating lesions in the CNS. Similar to previous studies (Brennan et al., 2001; Chataway et al., 1999; Nagra et al., 1997), we have found that MPO, being a key modulator of inflammation (Heinecke, 1999; Klebanoff, 1967; Klebanoff, 1970), is closely related to active demyelination. Additional biochemical assays indicate that MPO enzyme activity is markedly increased in active inflammatory lesions. Our histopathological results reveal extensive MPO infiltration, consistent with previous findings that MPO can transcytose after secretion (Baldus et al., 2001; Tiruppathi et al., 2004). These findings validate the approach of targeting MPO to monitor active inflammation and demyelination *in vivo*.

Both the DTPA(Gd) and the inactive MPO sensor have similar R1 relaxivity (both about 4.5 mM^{-1} s^{-1} at 1.5 T). Both conventional DTPA(Gd) and the MPO sensor reach the CNS through breakdown in the BBB. However, DTPA(Gd) relies on relatively large local concentrations to be detectable by MRI and also does not possess any tissue or molecular specificity (Bruck et al., 1997; Cotton et al., 2003). On the other hand, in a separate study, we have found that in mouse model of myocardial infarction, the MPO sensor was able to distinguish between wild type mice with full MPO expression, heterozygous MPO deficient mice with intermediate MPO expression, and MPO knockout mice with no MPO expression, thereby demonstrating high specificity to the enzyme myeloperoxidase (unpublished data). The increased lesion detection sensitivity and specificity seen on MPO imaging result from

MPO-mediated activation of the MPO sensor that leads to signal amplification and persistent enhancement in actively inflamed areas. The signal amplification would also allow improved detection of active lesions that cause subtle impairment of the BBB. Therefore, unlike conventional, nonspecific imaging agents, MPO imaging not only indicates BBB breakdown, but also the presence of actual inflammation. Specifically, MPO oxidizes the 5-hydroxytryptamide (5-HT) moieties on the MPO sensor into free radicals, which then combine to form oligomers up to 5 unites in length (Chen et al., 2006) and bind to proteins (Querol Sans et al., 2006). The resultant increase in molecular size and molecular dynamics generate a large increase in R1 relaxivity (shortened T1 relaxation time) and increase in MR signal intensity on T1-weighted MRI sequence (Chen et al., 2006). Furthermore, the larger molecular size and protein binding of the activated sensors cause retention of these products at sites of higher MPO activity, which has been confirmed by previous isotope studies (Chen et al., 2006; Querol Sans et al., 2005). However, because we found that the activated MPO sensor was cleared from the brain within 6 hours after administration, the protein-bound, activated MPO agents are likely digested and released by proteases that are present at sites of inflammation. While increasing the dose of DTPA(Gd) may increase lesion detection sensitivity, DTPA(Gd) cannot definitively confirm if the detected lesions represent active inflammation. Collectively, these properties of the MPO sensor allow earlier detection of active inflammatory, demyelinating lesions, and confirm areas of MPO activity noninvasively. The power of MPO imaging lies not only in its increased sensitivity from MPO-mediated signal amplification, but more importantly, in its ability to noninvasively confirm with high specificity the presence of pathology---that of elevated MPO activity and the presence of active inflammation.

We have shown that MPO imaging corresponds to areas of MPO expression and secretion, and represents regions of increased inflammation with macrophage/microglia infiltration, demyelination, and tissue disorganization. Interestingly, not all mac-3 positive cells (microglia/macrophages) contained MPO (Figure 4b). These cells may represent a subpopulation of macrophage/microglia that does not participate directly in inflammation (e.g., the M2 subpopulation) (Gordon, 2003; Mosser, 2003; Stein et al., 1992). Recently, several groups have demonstrated that ultrasmall superparamagnetic iron oxide (USPIO) nanoparticles can be used to noninvasively image macrophages in rodent EAE and human MS brains (Berger et al., 2006; Brochet et al., 2006; Dousset et al., 1999; Dousset et al., 2006; Floris et al., 2004; Rausch et al., 2003; Xu et al., 1998). It is likely that a combination of MPO imaging and macrophage imaging would allow the noninvasive identification and tracking of these different subpopulations of macrophages/microglia to further our understanding of their different roles in demyelinating diseases. While the current study used paramagnetic Gd in the MPO-sensitive chelator, it is possible to exchange the metallic cation for PET (^{64}Cu) or SPECT (^{111}In) detectable tracers. These comparative studies are ongoing and may offer additional insight into disease processes and further improve sensitivity. The MRI studies performed here had high spatial resolutions but were essentially identical to clinical pulse sequences. Thus, MPO imaging should be easily deployed in the community since no specialized pulse sequence or new equipment is needed.

Our results could have several implications in the clinical setting. MPO imaging could be useful to screen susceptible individuals in the presymptomatic stage, leading to earlier

treatment to decrease neurodegeneration and consequent morbidity. In addition, in established MS patients, MPO imaging could be used to better match clinical symptoms to improve relapse detection as well as more accurate temporal monitoring of active disease and therapeutic response. While this study used a higher dosage compared to the clinical human dose (0.3 mmol/kg vs. 0.1 mmol/kg for both DTPA(Gd) and MPO sensor), because mouse MPO is only about 10–20% as active as that of human MPO (Rausch and Moore, 1975), we expect that in humans the increase in sensitivity would be even more pronounced than demonstrated in our study. While formal toxicity and stability studies are on-going, preliminary data thus far revealed no adverse events in mice serially injected with five-fold the normal dose, and we found that the gadolinium chelation in the MPO sensor is more stable than that of DTPA(Gd) in zinc transmetallation assays (unpublished data). Therefore, enzymatic imaging targeting MPO points to a promising new technology for noninvasive confirmation of active inflammatory lesions in multiple sclerosis, potentially not only improve disease diagnosis and treatment assessment in the clinical setting, but may also lead to better evaluation of drug development and clinical trials of new therapies.

Acknowledgments

We thank the CMIR Chemistry Core (F. Reynolds and L. Josephson) for performing the chemical synthesis. We also thank C. Rangel, C. Kaufman, T. Sponholtz,V. Lok, and L. Stangenberg for experimental assistance.

Funding

National Institute of Health (R24-CA92782, R01-HL078641 to R.W.); the National Multiple Sclerosis Society (J.W.C.); the Dana Foundation (J.W.C.); the German National Academic Foundation and the Boehringer Ingelheim Fonds (M.O.B.).

Abbreviations

MPO	myeloperoxidase
MRI	magnetic resonance imaging
DTPA(Gd)	diethylenetriamine-pentaacetate gadolinium
5-HT-DTPA(Gd)	bis-5-hydroxytryptamide-diethylenetriamine-pentaacetate gadolinium
EAE	experimental autoimmune encephalomyelitis
BBB	blood-brain barrier
CNS	central nervous system
ROI	region of interest
PLP	proteolipid protein
MS	multiple sclerosis
R_1	longitudinal relaxivity
PBS	phosphate buffered saline
FITC	fluorescein isothiocyanate
CNR	contrast-to-noise ratio

SD	standard deviation
SEM	standard error of measurement
PET	positron emssion tomography
SPECT	single photon emission computed tomography

References

Baldus S, Eiserich JP, Mani A, Castro L, Figueroa M, Chumley P, et al. Endothelial transcytosis of myeloperoxidase confers specificity to vascular ECM proteins as targets of tyrosine nitration. J Clin Invest. 2001; 108:1759–1770. [PubMed: 11748259]

Berger C, Hiestand P, Kindler-Baumann D, Rudin M, Rausch M. Analysis of lesion development during acute inflammation and remission in a rat model of experimental autoimmune encephalomyelitis by visualization of macrophage infiltration, demyelination and bloodbrain barrier damage. NMR Biomed. 2006; 19:101–107. [PubMed: 16411166]

Bradley PP, Christensen RD, Rothstein G. Cellular and extracellular myeloperoxidase in pyogenic inflammation. Blood. 1982; 60:618–622. [PubMed: 6286012]

Brennan M, Gaur A, Pahuja A, Lusis AJ, Reynolds WF. Mice lacking myeloperoxidase are more susceptible to experimental autoimmune encephalomyelitis. J Neuroimmunol. 2001; 112:97–105. [PubMed: 11108938]

Brochet B, Deloire MS, Touil T, Anne O, Caille JM, Dousset V, et al. Early macrophage MRI of inflammatory lesions predicts lesion severity and disease development in relapsing EAE. Neuroimage. 2006; 32:266–274. [PubMed: 16650776]

Bruck W. The pathology of multiple sclerosis is the result of focal inflammatory demyelination with axonal damage. J Neurol. 2005; 252(Suppl 5):v3–v9. [PubMed: 16254699]

Bruck W, Bitsch A, Kolenda H, Bruck Y, Stiefel M, Lassmann H. Inflammatory central nervous system demyelination: correlation of magnetic resonance imaging findings with lesion pathology. Ann Neurol. 1997; 42:783–793. [PubMed: 9392578]

Chataway J, Sawcer S, Feakes R, Coraddu F, Broadley S, Jones HB, et al. A screen of candidates from peaks of linkage: evidence for the involvement of myeloperoxidase in multiple sclerosis. J Neuroimmunol. 1999; 98:208–213. [PubMed: 10430054]

Chen JW, Querol Sans M, Bogdanov AA Jr, Weissleder R. Imaging myeloperoxidase in mice using novel amplifiable paramagnetic substrates. Radiology. 2006; 240:473–481. [PubMed: 16864673]

Cotton F, Weiner HL, Jolesz FA, Guttmann CR. MRI contrast uptake in new lesions in relapsing-remitting MS followed at weekly intervals. Neurology. 2003; 60:640–646. [PubMed: 12601106]

Dousset V, Ballarino L, Delalande C, Coussemacq M, Canioni P, Petry KG, et al. Comparison of ultrasmall particles of iron oxide (USPIO)-enhanced T2-weighted, conventional T2-weighted, and gadolinium-enhanced T1-weighted MR images in rats with experimental autoimmune encephalomyelitis. AJNR Am J Neuroradiol. 1999; 20:223–227. [PubMed: 10094342]

Dousset V, Brochet B, Deloire MS, Lagoarde L, Barroso B, Caille JM, et al. MR imaging of relapsing multiple sclerosis patients using ultra-small-particle iron oxide and compared with gadolinium. AJNR Am J Neuroradiol. 2006; 27:1000–1005. [PubMed: 16687532]

Filippi M, Yousry T, Campi A, Kandziora C, Colombo B, Voltz R, et al. Comparison of triple dose versus standard dose gadolinium-DTPA for detection of MRI enhancing lesions in patients with MS. Neurology. 1996; 46:379–384. [PubMed: 8614498]

Floris S, Blezer EL, Schreibelt G, Dopp E, van der Pol SM, Schadee-Eestermans IL, et al. Blood-brain barrier permeability and monocyte infiltration in experimental allergic encephalomyelitis: a quantitative MRI study. Brain. 2004; 127:616–627. [PubMed: 14691063]

Frohman EM, Goodin DS, Calabresi PA, Corboy JR, Coyle PK, Filippi M, et al. The utility of MRI in suspected MS: report of the Therapeutics and Technology Assessment Subcommittee of the American Academy of Neurology. Neurology. 2003; 61:602–611. [PubMed: 12963748]

Frohman EM, Racke MK, Raine CS. Multiple sclerosis--the plaque and its pathogenesis. N Engl J Med. 2006; 354:942–955. [PubMed: 16510748]

Giovannoni G, Silver NC, Good CD, Miller DH, Thompson EJ. Immunological time-course of gadolinium-enhancing MRI lesions in patients with multiple sclerosis. Eur Neurol. 2000; 44:222–228. [PubMed: 11096222]

Gordon S. Alternative activation of macrophages. Nat Rev Immunol. 2003; 3:23–35. [PubMed: 12511873]

Greer JM, Sobel RA, Sette A, Southwood S, Lees MB, Kuchroo VK. Immunogenic and encephalitogenic epitope clusters of myelin proteolipid protein. J Immunol. 1996; 156:371–379. [PubMed: 8598487]

Heinecke JW. Pathways for oxidation of low density lipoprotein by myeloperoxidase: tyrosyl radical, reactive aldehydes, hypochlorous acid and molecular chlorine. Biofactors. 1997; 6:145–155. [PubMed: 9259996]

Heinecke JW. Mechanisms of oxidative damage by myeloperoxidase in atherosclerosis and other inflammatory disorders. J Lab Clin Med. 1999; 133:321–325. [PubMed: 10218761]

Imitola J, Chitnis T, Khoury SJ. Insights into the molecular pathogenesis of progression in multiple sclerosis: potential implications for future therapies. Arch Neurol. 2006; 63:25–33. [PubMed: 16401734]

Jacobs LD, Beck RW, Simon JH, Kinkel RP, Brownscheidle CM, Murray TJ, et al. Intramuscular interferon beta-1a therapy initiated during a first demyelinating event in multiple sclerosis. CHAMPS Study Group. N Engl J Med. 2000; 343:898–904. [PubMed: 11006365]

Kidd D, Barkhof F, McConnell R, Algra PR, Allen IV, Revesz T. Cortical lesions in multiple sclerosis. Brain. 1999; 122(Pt 1):17–26. [PubMed: 10050891]

Klebanoff SJ. A peroxidase-mediated antimicrobial system in leukocytes. J Clin Invest. 1967; 46:1078–1085.

Klebanoff SJ. Myeloperoxidase: contribution to the microbicidal activity of intact leukocytes. Science. 1970; 169:1095–1097. [PubMed: 4988715]

Klebanoff SJ, Waltersdorph AM, Rosen H. Antimicrobial activity of myeloperoxidase. Methods Enzymol. 1984; 105:399–403. [PubMed: 6328193]

Kutzelnigg A, Lucchinetti CF, Stadelmann C, Bruck W, Rauschka H, Bergmann M, et al. Cortical demyelination and diffuse white matter injury in multiple sclerosis. Brain. 2005; 128:2705–2712. [PubMed: 16230320]

MacKenzie-Graham A, Tinsley MR, Shah KP, Aguilar C, Strickland LV, Boline J, et al. Cerebellar cortical atrophy in experimental autoimmune encephalomyelitis. Neuroimage. 2006; 32:1016–1023. [PubMed: 16806982]

Merkler D, Boscke R, Schmelting B, Czeh B, Fuchs E, Bruck W, et al. Differential macrophage/microglia activation in neocortical EAE lesions in the marmoset monkey. Brain Pathol. 2006; 16:117–123. [PubMed: 16768751]

Miller D, Barkhof F, Montalban X, Thompson A, Filippi M. Clinically isolated syndromes suggestive of multiple sclerosis, part I: natural history, pathogenesis, diagnosis, and prognosis. Lancet Neurol. 2005; 4:281–288. [PubMed: 15847841]

Mosser DM. The many faces of macrophage activation. J Leukoc Biol. 2003; 73:209–212. [PubMed: 12554797]

Nagra RM, Becher B, Tourtellotte WW, Antel JP, Gold D, Paladino T, et al. Immunohistochemical and genetic evidence of myeloperoxidase involvement in multiple sclerosis. J Neuroimmunol. 1997; 78:97–107. [PubMed: 9307233]

Noseworthy JH, Lucchinetti C, Rodriguez M, Weinshenker BG. Multiple sclerosis. N Engl J Med. 2000; 343:938–952. [PubMed: 11006371]

Pomeroy IM, Matthews PM, Frank JA, Jordan EK, Esiri MM. Demyelinated neocortical lesions in marmoset autoimmune encephalomyelitis mimic those in multiple sclerosis. Brain. 2005; 128:2713–2721. [PubMed: 16150849]

Querol M, Chen JW, Weissleder R, Bogdanov A Jr. DTPA-bisamide-based MR sensor agents for peroxidase imaging. Org Lett. 2005; 7:1719–1722. [PubMed: 15844889]

Querol Sans M, Chen JW, Bogdanov AA Jr. A paramagnetic contrast agent with myeloperoxidase-sensing properties. Org Biomol Chem. 2006; 4:1887–1895. [PubMed: 16688334]

Querol Sans M, Chen JW, Weissleder R, Bogdanov AA Jr. Myeloperoxidase activity imaging using (67)Ga labeled substrate. Mol Imaging Biol. 2005; 7:403–410. [PubMed: 16292477]

Rausch M, Hiestand P, Baumann D, Cannet C, Rudin M. MRI-based monitoring of inflammation and tissue damage in acute and chronic relapsing EAE. Magn Reson Med. 2003; 50:309–314. [PubMed: 12876707]

Rausch PG, Moore TG. Granule enzymes of polymorphonuclear neutrophils: A phylogenetic comparison. Blood. 1975; 46:913–919. [PubMed: 173439]

Seeldrayers PA, Syha J, Morrissey SP, Stodal H, Vass K, Jung S, et al. Magnetic resonance imaging investigation of blood-brain barrier damage in adoptive transfer experimental autoimmune encephalomyelitis. J Neuroimmunol. 1993; 46:199–206. [PubMed: 8360329]

Stein M, Keshav S, Harris N, Gordon S. Interleukin 4 potently enhances murine macrophage mannose receptor activity: a marker of alternative immunologic macrophage activation. J Exp Med. 1992; 176:287–292. [PubMed: 1613462]

Storch MK, Bauer J, Linington C, Olsson T, Weissert R, Lassmann H. Cortical demyelination can be modeled in specific rat models of autoimmune encephalomyelitis and is major histocompatability complex (MHC) haplotype-related. J Neuropathol Exp Neurol. 2006; 65:1137–1142. [PubMed: 17146287]

Tiruppathi C, Naqvi T, Wu Y, Vogel SM, Minshall RD, Malik AB. Albumin mediates the transcytosis of myeloperoxidase by means of caveolae in endothelial cells. Proc Natl Acad Sci U S A. 2004; 101:7699–7704. [PubMed: 15136724]

Xu S, Jordan EK, Brocke S, Bulte JWM, Quigley L, Tresser N, et al. Study of Relapsing Remitting Experimental Allergic Encephalomyelitis SJL Mouse Model Using MION-46L Enhanced In Vivo MRI: Early Histopathological Correlation. J Neurosci Res. 1998; 52:549–558. [PubMed: 9632311]

Zakrzewska-Pniewska B, Styczynska M, Podlecka A, Samocka R, Peplonska B, Barcikowska M, et al. Association of apolipoprotein E and myeloperoxidase genotypes to clinical course of familial and sporadic multiple sclerosis. Mult Scler. 2004; 10:266–271. [PubMed: 15222689]

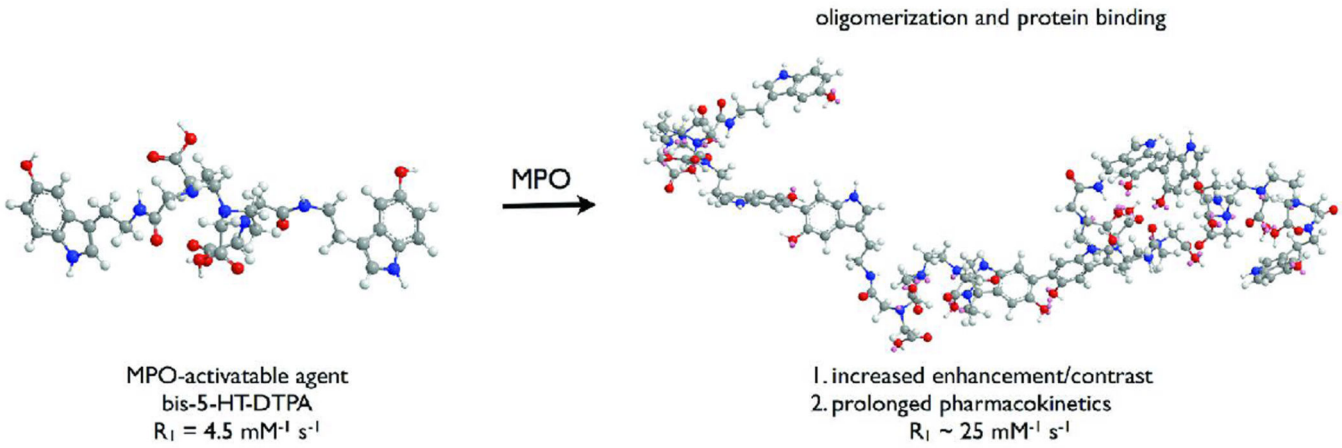

Figure 1.

Structure of the MPO agent and mechanism of action. In the presence of MPO, the agent is radicalized and form higher relaxivity oligomers, which can also bind to proteins.

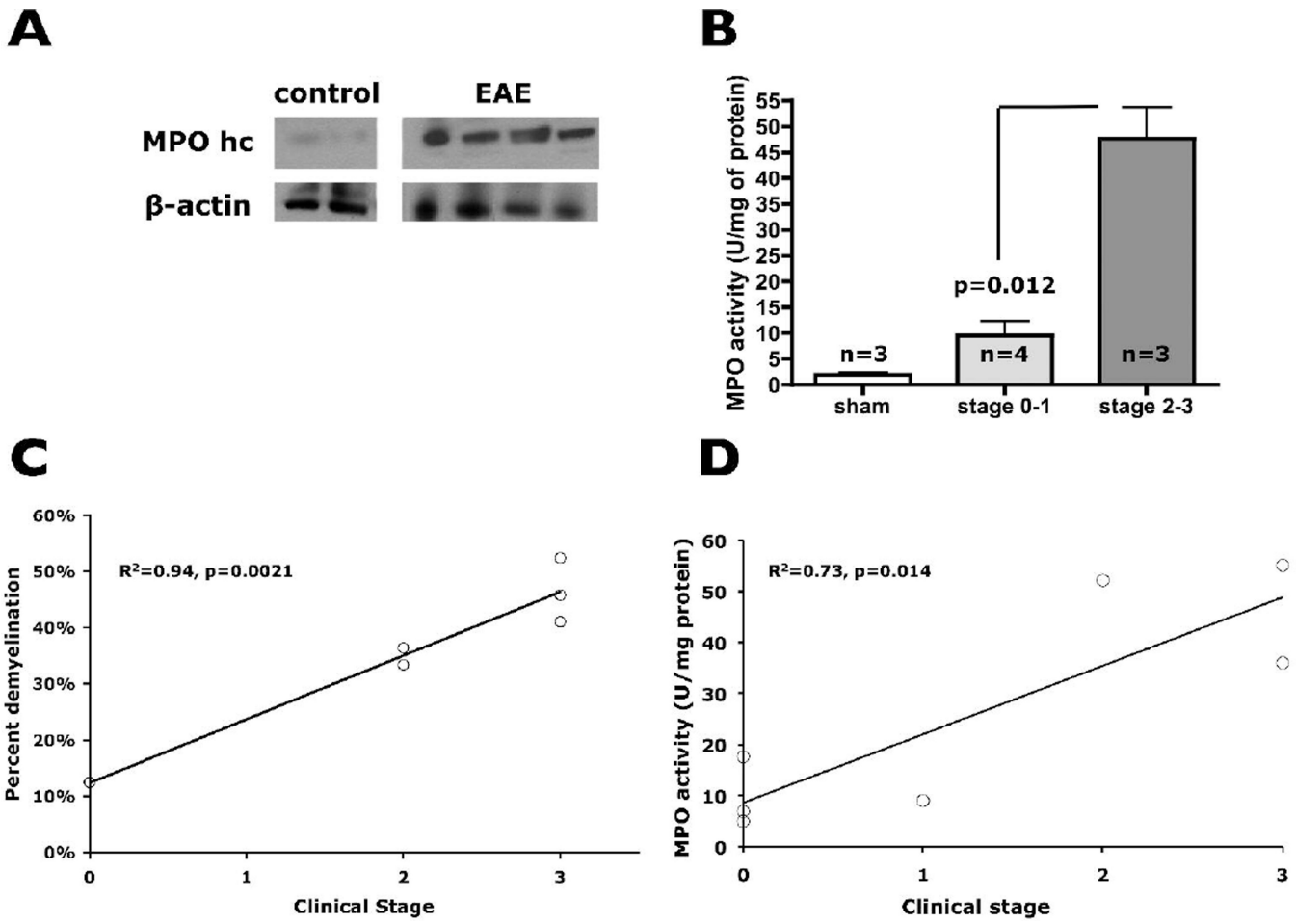

Figure 2.

MPO in EAE. (a) Western blotting confirmed the presence of MPO heavy chain in the brain specimen of mice induced with EAE. (b) Biochemical analysis of the MPO activity as a function of clinical staging demonstrated that higher clinical staging is associated with increased MPO activity. (c) There was increased demyelination at increasing clinilcal disease severity (R^2=0.94, p=0.0021). (d) MPO activity of each animal vs. its clinical disease stage. A positive correlation was found with R^2=0.73, p=0.014.

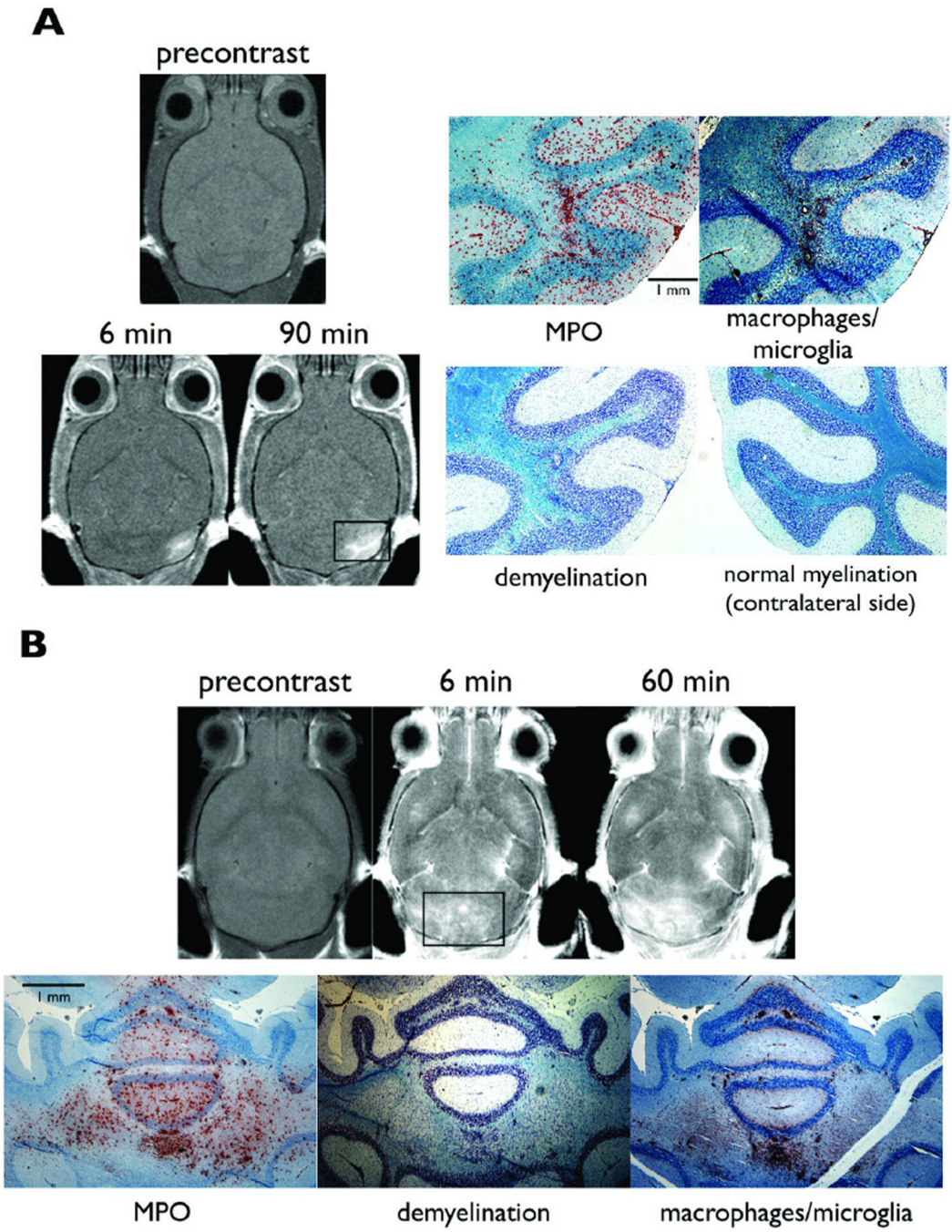

Figure 3.

MPO imaging and histopathological correlation. (a) shows a lesion in the cerebellum positive for the MPO sensor, and corresponded to MPO and macrophage/microglia positive areas on histopathology. Note the increased enhancement at 90 minutes compared to at 6 minutes. This lesion was detected by MPO imaging on day 5 after induction. Imaging was performed at 4.7 T. (b) shows a large area in the cerebellum with marked delayed enhancement that corresponded to areas positive for MPO and macrophages/microglia. The

areas of demyelination corresponded closely to MPO positive areas and areas exhibiting delayed enhancement on MPO imaging. Imaging was performed at 7 T.

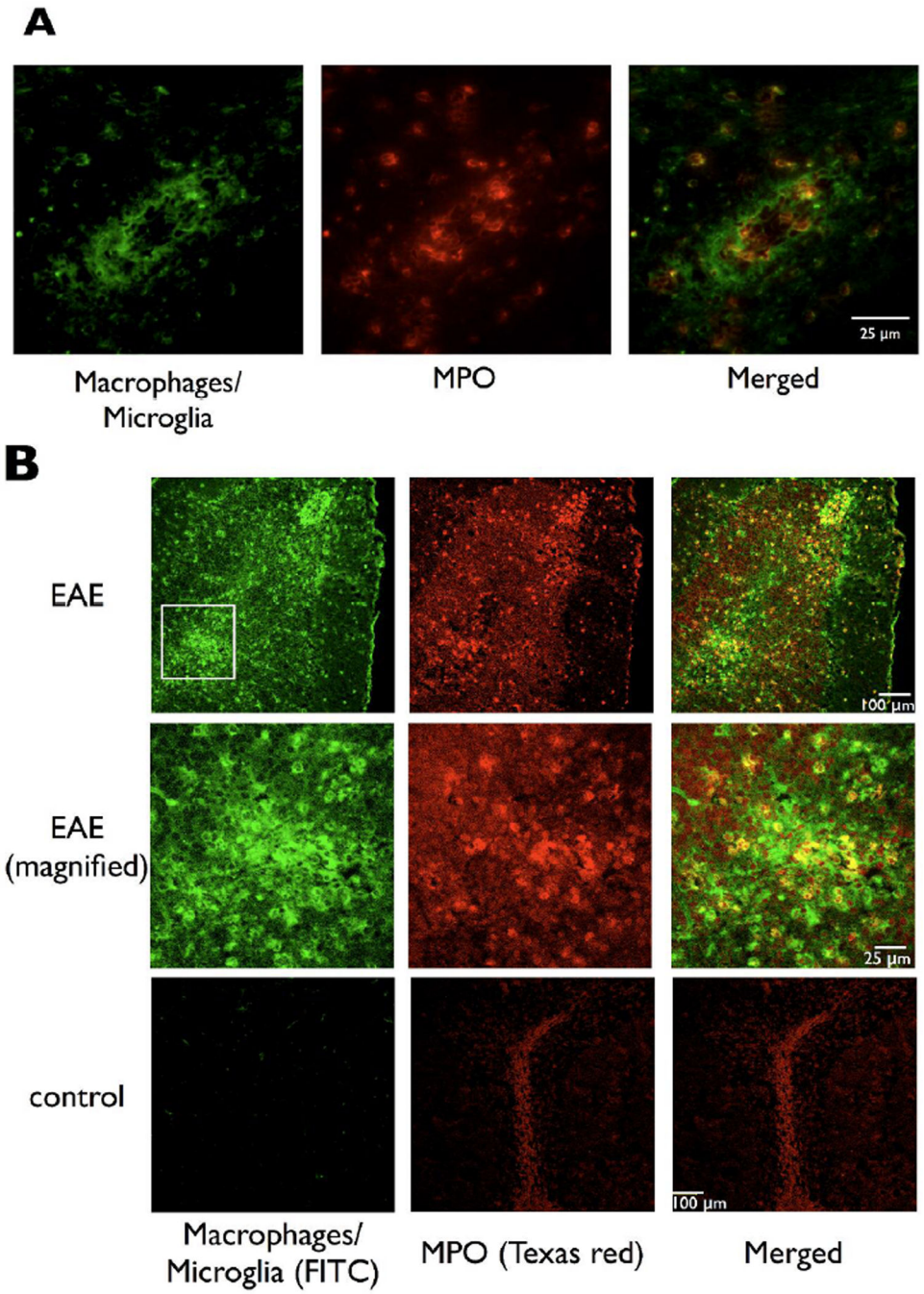

Figure 4.

Macrophages/microglia are the primary source of MPO. (a) Double immunofluorescence microscopy of a perivascular lesion shows that MPO co-localized with macrophages/microglia. (b) Confocal microscopy confirmed MPO correlated with macrophages/microglia. In addition, there was widespread architectural distortion in MPO positive areas.

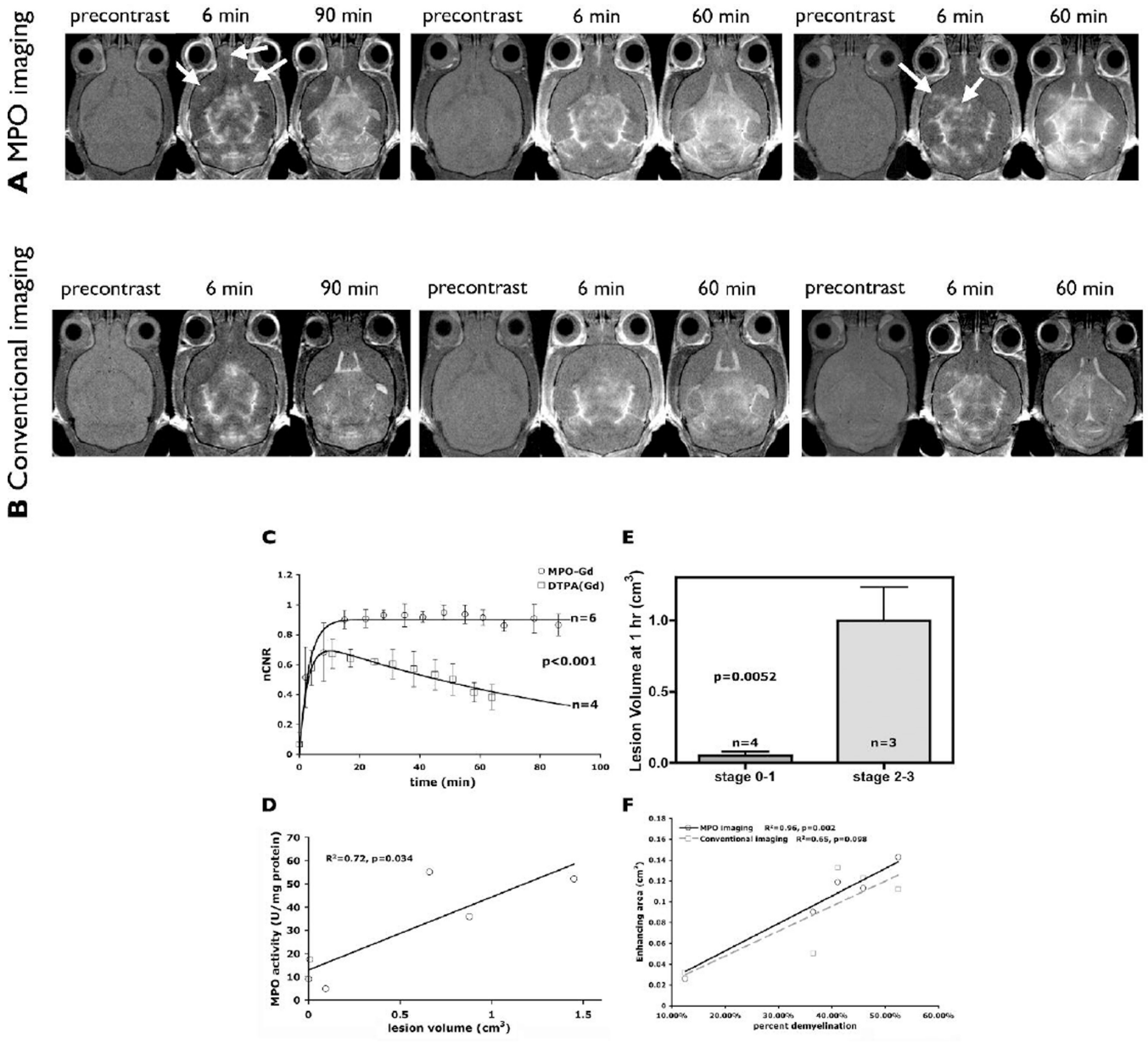

Figure 5.

Representative MPO vs. DTPA(Gd) imaging. Both MPO imaging and conventional imaging (top vs. bottom) represented the same animal at the same level. Three representative animals are shown. In the first two animals (left to right), conventional gadolinium was administered first followed by MPO sensor. In the last animal, the MPO sensor was administered first, followed by conventional gadolinium. (a) MPO imaging demonstrated more lesions on early post contrast images compared to conventional imaging, shown in (b). In addition, delayed enhancement confirmed MPO-mediated activation with the resultant prolonged pharmacokinetics. Arrows identify several focal active inflammatory lesions that are confirmed on the delayed MPO images. Note that some of the lesions detected by MPO imaging were either absent or barely perceptible, even retrospectively, on conventional DTPA(Gd) imaging. (b) Conventional DTPA(Gd) imaging for comparison. Imaging was

performed at 4.7 T. (c) Time course evaluations of normalized CNR (nCNR) revealed increased contrast enhancement and prolonged pharmacokinetics in mice EAE lesions when imaged with the MPO sensor compared to the nonspecific DTPA(Gd). (d) Lesion volume measured from delayed MPO imaging correlated with MPO activity (R^2=0.72, p=0.034). (e) Larger lesion volume measured on delayed MPO images corresponded to worse clinical disease. (f) Enhancing area from MPO imaging correlated significantly better with percent demyelination (solid black line, R^2=0.96, p=0.002) than did conventional imaging (dashed gray line, R^2=0.65, p=0.098).

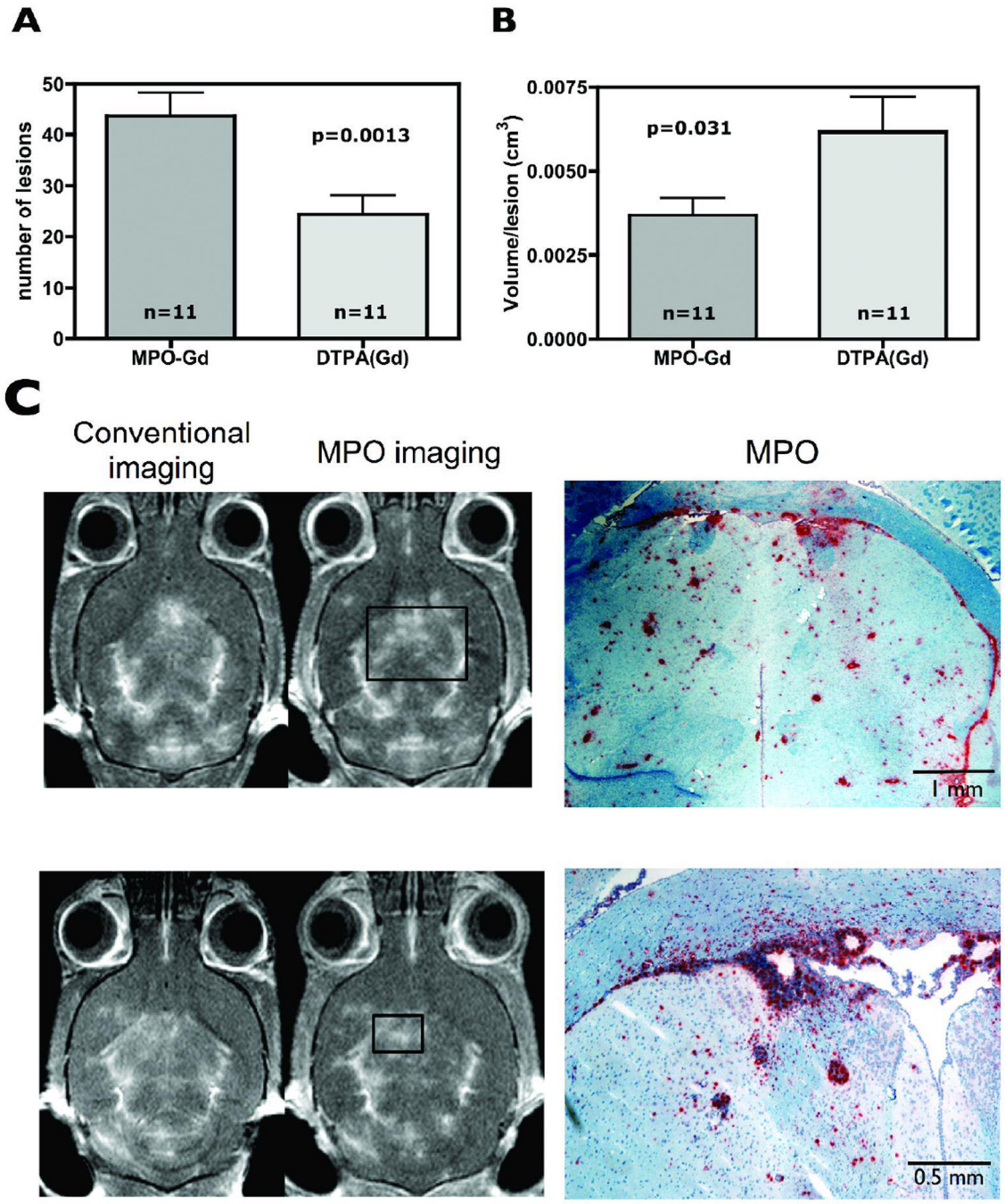

Figure 6.

MPO imaging increases lesions detection sensitivity. (a) MPO imaging detected more lesions, and (b) MPO imaging detected smaller lesions. (c) Correlative MPO histopathology to imaging for the first and third mice shown in Figure 5 illustrates the increased lesion sensitivity of MPO imaging compared to conventional imaging.